ADVANCED
FUNCTIONAL
MATERIALS
www.afm-journal.de

Materials
Views
www.MaterialsViews.com

FULL PAPER

Rapid Self-Assembly of Macroscale Tissue Constructs at Biphasic Aqueous Interfaces

John P. Frampton, Brendan M. Leung, Eve L. Bingham, Sasha Cai Lesher-Perez, Jack D. Wang, Hady T. Sarhan, Mohamed E. H. El-Sayed, Stephen E. Feinberg, and Shuichi Takayama*

An entirely new approach to tissue engineering is presented that uses the interfacial forces between aqueous solutions of phase-separating polymers to confine cells and promote their assembly into interconnected, macroscopic tissue constructs. This simple and inexpensive general procedure creates free-standing, centimeter-scale constructs from cell suspensions at the interface between poly(ethylene glycol) and dextran aqueous two-phase systems in as little as 2 h. Using this method, skin constructs are produced that integrate with decellularized dermal matrices, on which they differentiate and stratify into skin equivalents. It is demonstrated that the constructs produced by this method have appropriate integrity and mechanical properties for use as in vitro tissue models.

1. Introduction

While there are many pre-existing strategies for fabricating and printing biomaterial scaffolds and hydrogels laden with low densities of cells,[1] many tissues are predominantly comprised of cells with minimal material separating the cells. Currently, methods to prepare such scaffold-free, cell-only constructs are limited to iterative assembly of spheroids into aggregates,[2] magnetic levitation culture of artificially magnetized cells,[3] or temporary formation of cell sheets,[4] all of which have inherent limitations. One of the most frequently used approaches for fabricating cell-rich constructs is the use of poly(N-isopropylacrilamide) (NIPAM)-modified thermoresponsive substrates.[4] NIPAM-modified substrates promote cell adhesion at physiological temperatures (≈37 °C) and release cells when the temperature is lowered below 22 °C. However, this technology requires that cells be grown for a period of at least several days to establish the appropriate cell–cell connections, requires extensive and costly cell substrate engineering, and can fail if appropriate temperature conditions are not met. These requirements present potential limitations when rapid treatment is needed.

Research on in vitro organ models and tissue replacement therapies,[5] therefore, would benefit from a faster, simpler, and less-expensive general procedure that can create macroscopic cell-only constructs. We developed a new approach that meets these general demands by assembling multiple types of cell suspensions into free-standing, centimeter-scale constructs at the interface between phase-separating aqueous solutions containing poly(ethylene glycol) and dextran[6,7] in as little as 2 h. Our cell construct formation method is complementary to NIPAM-engineered cell sheets and other methods for cell construct fabrication, while providing advantages in terms of the speed at which the constructs form (several hours), the relative simplicity of the procedure, the range of cell types that can be used, and cost effectiveness.

Prof. J. P. Frampton, H. T. Sarhan
School of Biomedical Engineering
Dalhousie University
Halifax, NS B3H 4R2, Canada
Dr. B. M. Leung, S. C. Lesher-Perez, Dr. J. D. Wang,
Prof. M. E. H. El-Sayed, Prof. S. Takayama
Department of Biomedical Engineering
University of Michigan
Ann Arbor, MI 48109, USA
E-mail: takayama@umich.edu
E. L. Bingham, Prof. S. E. Feinberg
Department of Oral and Maxillofacial Surgery
University of Michigan
Ann Arbor, MI 48109, USA
Prof. S. Takayama
Department of Macromolecular Science and Engineering
University of Michigan
Ann Arbor, MI 48109, USA
Dr. B. M. Leung, S. C. Lesher-Perez, Prof. S. Takayama
Biointerfaces Institute
University of Michigan
Ann Arbor, Michigan 48108, USA

2. Results and Discussion

2.1. Rapid Self-Assembly of Cell-Only Constructs

The straightforward three-step procedure for assembling the constructs (**Figure 1**a) starts with partial filling of an appropriate vessel (e.g., a microcentrifuge tube) with cell culture medium containing dextran (DEX). Next, cells suspended in culture medium containing poly(ethylene glycol) (PEG) are layered
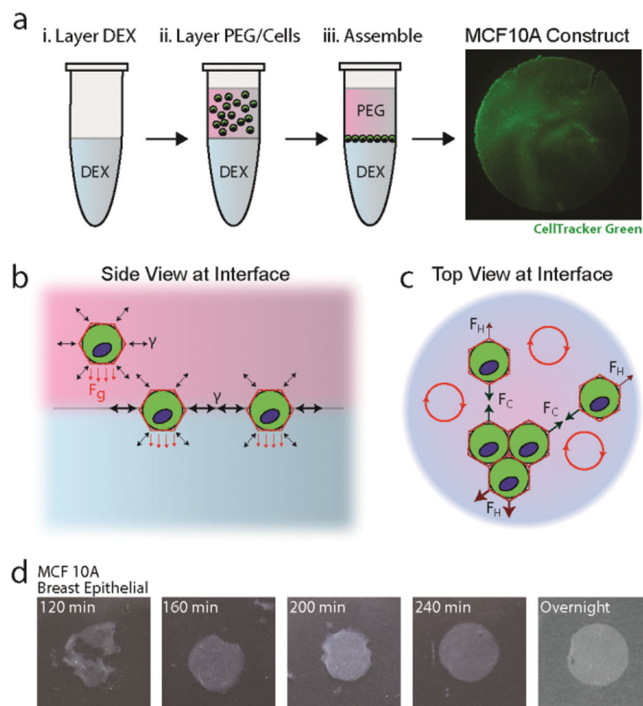
Figure 1. Planar tissue constructs assemble rapidly at biphasic aqueous interfaces. a) A suspension of cells in poly(ethylene glycol) (PEG) medium is layered on a solution of dextran (DEX) to form an aqueous two-phase system (ATPS). The geometrically flat PEG–DEX interface supports self-assembly of cells into macroscopic planar constructs. b) Over the course of approximately 15 min, the cells settle by gravity (F_g, red arrows) to the PEG–DEX interface. Once at the interface, interfacial tension (γ, blue arrows) and buoyancy from the heavier DEX phase pin the cells in the x–y plane and prevent them from falling to the bottom of the tube. c) At the interface, lateral cell movements are influenced by capillary attractive forces (F_C) and hydrostatic resistance to movement (F_H), as well as by advective/convective currents (red circular arrows). After ≈15 min, the PEG–DEX interface is completely populated by cells, restricting the lateral movement of individual cells. d) This simple process facilitates the formation of cell–cell connections, leading to the self-assembly of planar constructs that are robust to manipulation in as little as 120 min, although the cells can be maintained at the liquid–liquid interface for 12 h or longer. MCF10A construct diameters in (a) and (d) are ≈9.0 mm.

on top of the DEX medium. This forms an aqueous two-phase system (ATPS), where the PEG and DEX phases are immiscible. The final step is cellular self-assembly. During the first ≈15 min, the cells settle and collect at the interface between the DEX and PEG (Figure 1b) due to density differences and interfacial forces[6,8] between the denser DEX phase and the PEG phase. Importantly, the DEX solution–PEG solution tube interface is quite flat, whereas a curved meniscus will form with solution–air–tube interfaces. As cells collect at this flat, biphasic aqueous interface, capillary attraction,[9] hydrostatic resistance to movement,[9] diffusiophoretic effects due to equilibration between the two polymer phases,[10] convection/advection,[11] and Marangoni propulsion[12] (Figure 1c) influence lateral cell movement. As the x–y plane (i.e., the biphasic aqueous interface) becomes populated by cells, however, cell movement becomes more restricted. Over several hours, cell–cell contacts strengthen sufficiently to produce a self-assembled macroscopic planar cell construct that can withstand handling, washing, and

transport. For some cell types (e.g., MCF10A human mammary epithelial cells and keratinocytes), robust constructs are formed within 120–160 min of incubation (Figure 1d).

The ability to form tissue constructs at the biphasic aqueous interface is dependent on both the physicochemical properties of the ATPS[6,8] and the properties of the cells. We estimated the number of cells required to populate the interface of a 1.5 mL microcentrifuge tube with 1–2 layers of cells to be ≈1×10^6 based on the approximate circumferential area of a trypsinized cell (5–10 μm^2) and the area of the biphasic aqueous interface (≈66.5 mm^2). Using 1×10^6 cells as a reference cell seeding number, we varied the concentrations of DEX and PEG to optimize the construct morphology and maximize the cell viability (Figure S1, Supporting Information). A 10% DEX solution overlaid with a 5% PEG system gave the best construct formation based on macroscopic morphologies (e.g., intact constructs vs incomplete constructs or rings of cells). When the polymer concentration was not high enough (or when an ATPS did not form), many of the cells sank through the interface to the bottom of the microcentrifuge tube. Cell viability was greater than 80% for all tested ATPS formulations after dissociation of the constructs in trypsin, with the exception of the DEX 10%/PEG 2.5% system (75%), the DEX 15%/PEG 10% system (78%), and the DEX 30%/PEG10% system (58%) (Figure S2, Supporting Information).

The ability to form stable macroscopic structures was also cell type dependent (**Figure 2**a). Epithelial cell types (e.g., MCF10A, lung (A549), kidney (MDCK), and primary human keratinocytes) formed robust constructs with cells interconnected by adherens junctions, as indicated by MCF10a construct E-cadherin staining (Figure S3a, Supporting Information), while HepG2 C3A cells formed weak constructs. In contrast, HeLa cells did not form stable constructs at all. The HeLa cells disaggregated when removed from the DEX–PEG interface, because HeLa cells have altered expression of cell–cell adhesion proteins, such as E-cadherin.[13] Additionally, thicker multilayer constructs with distinct layers of differently labeled cells could be formed by applying two or more populations of cells sequentially at intervals of at least 15 min (Figure 2b).

2.2. Formation of Skin Equivalents following Rapid Keratinocyte Self-Assembly

To examine the potential use of the keratinocyte constructs as tissue replacements, we tested their integration and differentiation on AlloDerm. AlloDerm is derived from decellularized human skin, containing nearly intact extracellular matrix.[14] It is one of the leading implantable tissue matrices for soft tissue regeneration due to its ability to promote cell repopulation and revascularization at surgical sites. AlloDerm can also be used as a model matrix to examine integration of cell-based therapies.

After transplanting the constructs from the liquid–liquid interface culture system to the AlloDerm substrate, the constructs were maintained in submersion culture followed by air–liquid interface culture. At various time points in this culture process, the constructs (and underlying AlloDerm) were fixed and sectioned for H&E staining and immunohistochemistry. After 3 days of submersion culture, the constructs showed signs
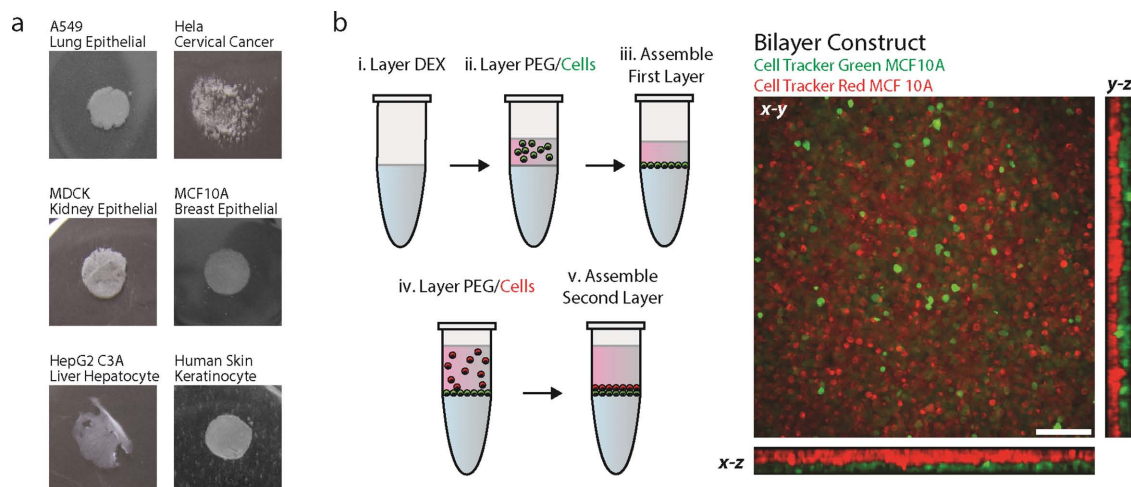
Figure 2. Self-assembled planar tissue constructs can be produced with various cell types and configurations. a) Cell types of various origins, including A549, MDCK, MCF10A, HepG2 C3A, and primary skin cells (but not HeLa cells), are capable of assembling into macroscopic planar constructs. Construct diameters are ≈9.0 mm. b) Bilayer constructs can be formed by seeding the cells sequentially in intervals of at least 15 min using separate volumes of PEG, as revealed by confocal imaging of CellTracker-labeled constructs. Scale bar is 100 μm.

of integration with the AlloDerm, as indicated by the cell morphologies and bluish-purple coloration of cells at the interface between the construct and the AlloDerm (**Figure 3**a). After an additional 5 days of air–liquid interface culture, the cells in contact with the AlloDerm continued to proliferate, while forming a stratified eosinophillic layer of cells that was mostly devoid of nuclei (Figure 3b). At both time points in culture, there was an additional layer of cells present that did not contribute to

integration, but that also did not appear to interfere with cell differentiation and stratification. In addition, the cells in contact with the AlloDerm expressed CD44 (Figure 3c), a cell-surface glycoprotein that binds hyaluronic acid to promote cell–cell interactions in developing skin tissue.[15] The cells residing above the CD44+ layer, closer to the air interface, expressed filaggrin (Figure 3d), a protein that binds keratin in the stratum corneum that is indicative of epithelial differentiation.[16] These immunohistochemical data, along with additional immunofluorescence staining data for E-cadherin, occludin, and laminin gamma 2 (Figure S3b, Supporting Information), suggest that our method has potential applications in formation of structurally appropriate skin equivalents.

2.3. Characterization of Cell-Only Constructs as Tissue Models

To further demonstrate the integrity of the cell-only constructs and provide data to support their potential use as in vitro tissue models, we measured the transepithelial electrical resistance (TEER) for the most rapidly forming construct (MCF10A) (**Figure 4**a,b). TEER can be used to assess the integrity (i.e., the permeability) of cell monolayers and tissues by measuring the flow of electrical current across the specimen. Higher TEER typically correlates with higher expression of intercellular junction proteins.[17] The TEER values for the MCF10A constructs formed by self-assembly at the biphasic aqueous interface for 4 h with subsequent transfer to Transwell membranes were significantly higher than the TEER values for Transwell
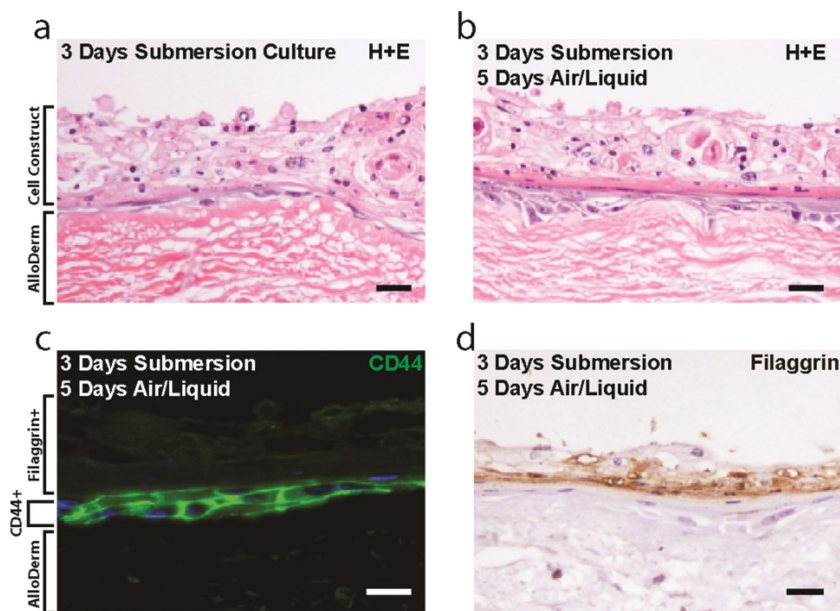

Figure 3. Constructs formed from primary human keratinocytes are capable of forming skin-like structures on decellularized dermal matrices. a) H&E staining of a keratinocyte construct after 3 days of submersion culture showing conformal attachment of the construct to the surface of the AlloDerm matrix. b) H&E staining of a keratinocyte construct after 3 days of submersion culture and 5 days of air–liquid interface culture showing stratification of the construct above the AlloDerm matrix. c) Cells in contact with the AlloDerm express CD44, a marker for developing/proliferating skin cells. d) The stratified cell layer above the CD44-positive cell layer expresses filaggrin, a marker for keratinocyte differentiation. Scale bars are ≈20 μm.
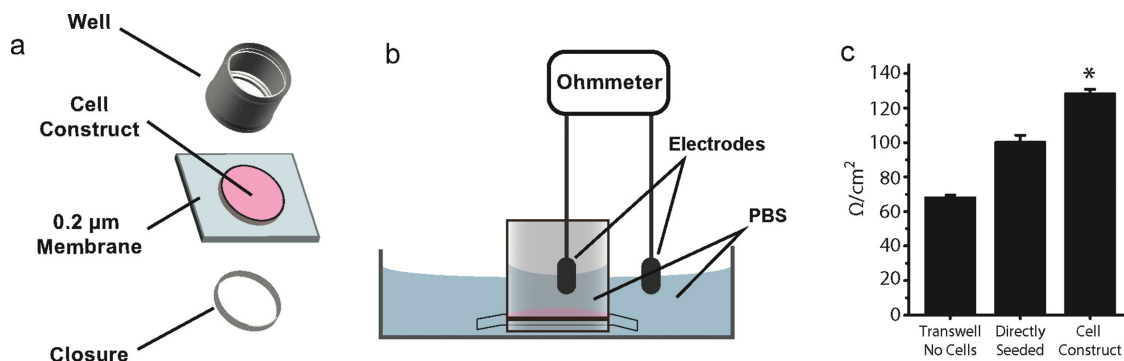
Figure 4. Trans-epithelial electrical resistance (TEER) measurements of construct barrier integrity. a) A construct resting on a 0.2 μm pore size Transwell membrane is sandwiched between the two components of a CellCrown insert. b) Once assembled, the TEER is measured using chopstick electrodes placed inside and outside of the CellCrown insert. c) The TEER data suggest that MCF10A constructs form more robust interconnections (resulting in significantly lower permeability and higher electrical resistance) than MCF10A cells seeded directly on 2D rigid Transwell membrane supports. Error bars represent the standard error of the mean for $n \geq 6$ samples per condition. The asterisk represents $p < 0.001$ versus the directly seeded cells and the Transwell alone by one-way ANOVA with Holm–Sidak multiple comparisons test.

membranes that were directly seeded with the same number of cells and cultured for 4 h (Figure 4c). This suggests that culturing cells at liquid–liquid interfaces promote the formation of cell–cell junctions, leading to epithelial constructs with enhanced barrier properties. It is possible, that the lack of cell-substrate interactions leads to a greater potential for the formation of cell–cell connections, whereas when cells are cultured directly on a support membrane, cell–substrate interactions dominate at the expense of cell–cell contacts, at least at early time points in culture.

We also characterized the mechanical properties of the MCF10A constructs using a custom mechanical burst testing device (**Figure 5**a–c). This system measured the mechanical properties of the constructs exposed to air pressure, while maintaining them in a liquid environment consisting of cell culture medium to ensure their viability. Based on the pressure–strain data obtained using this system, we determined the average bursting pressure to be 0.14 kPa, with failure typically occurring between 350% and 400% strain (Figure 5d). We calculated the average ultimate tensile strength of the MCF10A construct to be 10.6 kPa from the burst pressures together with

the shape of the constructs at bursting. The construct strength was lower than what is typically observed for mature tissues, but this was expected because the cells in the constructs had only a short period of 24 h before testing, an insufficient time to produce extracellular matrix components that contribute to tissue strengthening. The observed strain at bursting was larger than other elastic biological tissues, such as lung epithelium[18] and thin-film elastomeric biomaterials.[19] The relatively large strain values at bursting for our constructs can be explained by stretching of the cells at their connection points (e.g., from initial 10 μm-diameter spheres to 30 μm-diameter ellipsoids). In addition, in areas where more than one layer of cells is present, it may be possible for cells to slide across one another before the construct ultimately fails, leading to larger than expected strain values.

3. Conclusions

Based on our characterization data, the use of biphasic aqueous interfaces seems to be uniquely suited for rapid assembly of
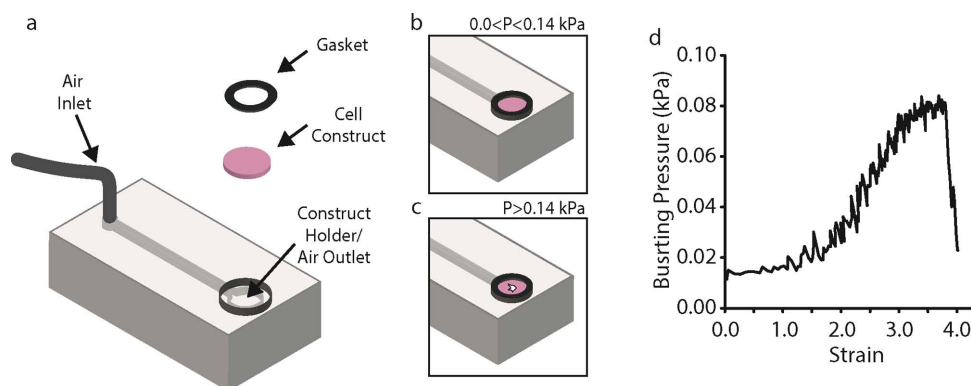

Figure 5. Analysis of construct mechanical properties by way of microfluidic burst pressure testing. a) A construct is placed in the outlet/holder region of the two-layer device and held in place by a PDMS gasket. An air plug is introduced via the air inlet to apply pressure to the construct. b) From 0.0 to ≈0.14 kPa of applied pressure constructs stretch, but remain intact. c) At applied pressures above ≈0.14 kPa the constructs rupture. d) Pressure–strain curve for an MCF10A construct tested on the custom microfluidic mechanical testing device. For $n = 4$ tested constructs, the average burst pressure was 0.14 kPa with a standard error of 0.04 and the average ultimate tensile strength was 10.6 kPa with a standard error of 3.

macroscopic planar tissue constructs. These cell-supporting interfaces, comprised predominantly of cell culture medium with small amounts of biocompatible polymers, not only collect cells into a tight plane, but also promote the cellular processes that form intercellular junctions. Importantly, the cell assembly process is simple, inexpensive, requires no specialized equipment, and should be accessible to any lab. Our mechanical characterization and experience handling the constructs demonstrate surprising mechanical robustness of these rapidly assembled, cell-only constructs. Moreover, the unprecedented speed with which these macroscopic planar constructs can be assembled is not only convenient for constructing tissue models, but may also provide advantages for regenerative medicine where rapid point-of-care assembly of cells into constructs can be beneficial.[20]

For many tissue replacement therapies, cell-based constructs can provide greater functionality than cell-free constructs.[21] While, NIPAM-engineered substrate can produce cell sheets that can be applied for treatment of damage to epithelial or other tissues,[22] this technology requires that cells be grown for a period of at least several days for cells to establish the appropriate connections. Our cell construct formation method, on the other hand, is rapid, requiring only hours to produce a construct from a cell suspension. The keratinocyte constructs we produced were capable of integrating with a dermal matrix, differentiating and stratifying into multiple epidermal layers. In addition, our method works with many other cell types, even those that form relatively weak cell–cell connections, opening up the possibility for applications beyond epithelial tissue engineering. Furthermore, while this paper focuses mainly on human cell applications, the concept of biphasic aqueous interface assembly may find broader use in biology as well as non-biological applications.[23]

4. Experimental Section

Polymer Systems: Dextran (DEX; MW 500 000 g mol−1; Pharmacosmos, Holbaek, Denmark) and poly(ethylene glycol) (PEG; MW 35 000 g mol−1; Sigma, St. Louis, MO) were dissolved in cell-type specific culture medium at final concentrations (without DEX–PEG equilibration) ranging from 10–30 wt% DEX and 2.5–10 wt% PEG on a rotary shaker overnight. The polymer solutions were used the following day for construct formation.

Cell Culture: A549, MDCK, HepG2 C3A, and HeLa cells were propagated prior to construct fabrication in DMEM containing 10% FBS and 1% anti–anti solution. MCF10A cells were propagated in MEGM BulletKit medium (CC-3150, Lonza, Allendale, NJ). Primary human keratinocytes were isolated from discarded human skin from mastectomy surgeries following informed consent using established procedures[24] and propagated in EpiLife medium (Life Technologies, Carlsbad, CA). All cells were maintained in a humidified incubator at 37 °C and 5% CO_2. One day prior to construct formation, at approximately 90% confluence, the cells were split and replated to approximately 70% confluence.

Construct Fabrication: One day after subculture, the cells were trypsinized, counted, and resuspended at 2×10^6 cells in PEG. The DEX solutions (500 µL per tube) were dispensed into microcentrifuge tubes. The PEG cell suspensions (500 µL per tube) were then layered on top of the DEX solutions in the microcentrifuge tubes to form aqueous two-phase systems (ATPSs) containing 1×10^6 cells. The microcentrifuge tubes were then incubated in a humidified incubator at 37 °C and 5% CO_2 for up to 24 h. To remove the constructs from the microcentrifuge tubes,

the contents of the tubes were gently poured into 35 mm culture dishes containing fresh culture medium. To fabricate multilayer constructs, two or more cell populations were dispensed into the microcentrifuge tubes at intervals of at least 15 min to allow the previous aliquot of cells to become captured at the ATPS interface. Two populations of MCF10A cells labeled with Red and Green Cell Tracker dyes (Life Technologies) were used to demonstrate bilayer-type constructs.

Transepithelial Electrical Resistance (TEER): TEER chambers were assembled using 0.20 µm pore size membranes (Millipore, Billerica, MA) and CellCrown cell culture insert assemblies (Scaffdex, Tampere, Finland) (Figure 4 a,b). Cells were seeded on pre-assembled CellCrown inserts at a density of 1×10^6 cells/insert at the time of construct assembly. After construct formation, the constructs were placed on the Millipore membranes, which were then snapped together within the CellCrowns to enclose the constructs. The TEER values of the pre-seeded and construct specimens were then measured using standard chopstick electrodes (World Precision Instruments, Sarasota, FL) and normalized by surface area.

Mechanical Testing: The constructs were placed over the outlet of a microfluidic channel submerged in cell culture medium (Figure 5a–c). The cell construct was held in place by a PDMS gasket with downward applied pressure. A syringe pump (Model KDS220, KD Scientific, Holliston, MA) was used to provide constant volumetric flow into the device. An air plug was placed within the microfluidic channel to produce an applied force on the construct with a constant volumetric inflow rate of 100 µL min−1. The applied pressure was measured using pressure sensors (Model 142PC05D, Honeywell, NJ, USA) that were in-line with the device inlets via rigid Tygon tubing (Saint-Gobain Tygon R-3603 Clear Laboratory Tubing, Saint-Gobain Performance Plastics, Akron, OH). The source pressure was measured as a constant volumetric inflow was applied, causing the air plug to displace the construct. Data were obtained at a sampling rate of 1000 Hz with 1 data point recorded every 100 ms in LabView. Prior to applying a constant volumetric inflow rate, a baseline measurement was taken without the construct to serve as a control for device performance. Additionally, we measured the pressure accumulation for a constant volumetric inflow rate within a closed, nondeformable microfluidic channel. This measurement allowed us to extrapolate the deformation of the construct from the pressure difference between the closed system and the construct by assuming that the pressure difference was proportional to the displaced volume of the construct. We also assumed that under applied pressure, the construct behaved as a homogeneous material (i.e., it expanded to form a spherical cap). We determined the change in height for the spherical cap, by using the known base of the cap and the displaced volume of the cap according to

$$V = \frac{\pi h}{6}\left(3a^2 + h^2\right) \tag{1}$$

where V is the volume, a is the known base of the cap, and h is the cap height. Applying the change in height, we then calculated the surface area of the construct according to

$$A = \pi\left(a^2 + h^2\right) \tag{2}$$

and used the radial expansion of the surface area of the expanded spherical cap to determine the strain rate. An additional assumption was that the air bubble used to apply the pressure did not diffuse or dissipate significantly through the construct. To determine ultimate tensile strength, we calculated the hoop stress for a thin-walled spherical vessel at the time of rupturing using

$$\text{stress} = \frac{Pr}{2t} \tag{3}$$

where P is the bursting pressure, r is the radius at the time of bursting, and t is the thickness of the cell construct at bursting. We assumed that the cell construct thinned out as it was stretched, but used conservation of volume to calculate the change in thickness as it thinned. The initial thickness used to calculate the ultimate strength was 70 µm, which was the approximate thickness of the cell constructs formed after 24 h.

Dermal Integration Assay: AlloDerm decellularized tissue matrices (LifeCell, Bridgewater, NJ) were used to test keratinocyte construct integration and differentiation. After construct formation, the keratinocyte constructs were placed on AlloDerm scaffolds, which were then placed on Transwell inserts with cell culture medium supplied from beneath for 1 day of air–liquid culture to allow the constructs to attach to the AlloDerm. The following day, the constructs were placed in submersion culture for 3 days with daily medium exchange. After 3 days, the constructs were returned to air-liquid interface culture for an additional 5 days with medium exchanged daily.

Histology and Immunostaining: Sectioning and H&E staining of formalin-fixed, paraffin-embedded samples were performed by the Histology Core at the University of Michigan, School of Dentistry. Sections that were not stained by H&E were probed for immunofluorescence detection using a CD44 antibody produced in rabbit with an Alexa-488 goat anti-rabbit secondary antibody (both from Sigma, St. Louis, MO) and counterstained with Hoechst 33342. Other sections were probed for chromogenic detection using an HRP-conjugated anti-filaggrin antibody.

Microscopy and Imaging: Confocal images of CellTracker Green- and Red-labeled cells were acquired on a Nikon A1 Spectral Confocal System (Nikon Instruments Inc., Melville, NY). Color images were acquired on a Nikon Eclipse Ci system. All other fluorescence images were acquired on Nikon TE300 system. Macroscopic images of unlabeled living constructs were acquired using a Nikon DLSR Digital Camera.

Supporting Information

Supporting Information is available from the Wiley Online Library or from the author.

Acknowledgements

[1] a) M. W. Tibbitt, K. S. Anseth, *Biotechnol. Bioeng.* **2009**, *103*, 655; b) D. Seliktar, *Science* **2012**, *336*, 1124.

[2] E. Fennema, N. Rivron, J. Rouwkema, C. van Blitterswijk, J. de Boer, *Trends Biotechnol.* **2013**, *31*, 108.

[3] G. R. Souza, J. R. Molina, R. M. Raphael, M. G. Ozawa, D. J. Stark, C. S. Levin, L. F. Bronk, J. S. Ananta, J. Mandelin, M. M. Georgescu, J. A. Bankson, J. G. Gelovani, T. C. Killian, W. Arap, R. Pasqualini, *Nat. Nanotechnol.* **2010**, *5*, 291.

[4] K. Matsuura, R. Utoh, K. Nagase, T. Okano, *J. Controlled Release* **2014**, *190*, 228.

[5] E. S. Place, N. D. Evans, M. M. Stevens, *Nat. Mater.* **2009**, *8*, 457.

[6] P. Å. Albertsson, *Partition of Cell Particles and Macromolecules*, Wiley, New York **1986**.

[7] a) H. Tavana, S. Takayama, *Biomicrofluidics* **2011**, *5*, 13404; b) J. P. Frampton, Z. Z. Fan, A. Simon, D. Chen, C. X. Deng, S. Takayama, *Adv. Funct. Mater.* **2013**, *23*, 3420.

[8] Y. G. Liu, R. Lipowsky, R. Dimova, *Langmuir* **2012**, *28*, 3831.

[9] a) N. D. Vassileva, D. van den Ende, F. Mugele, J. Mellema, *Langmuir* **2005**, *21*, 11190; b) M. P. Boneva, N. C. Christov, K. D. Danov, P. A. Kralchevsky, *Phys. Chem. Chem. Phys.* **2007**, *9*, 6371.

[10] T. Ban, T. Yamada, A. Aoyama, Y. Takagi, Y. Okano, *Soft Matter* **2012**, *8*, 3908.

[11] K. Vijayakumar, S. Gulati, A. J. deMello, J. B. Edel, *Chem. Sci.* **2010**, *1*, 447.

[12] a) T. Ban, T. Yamagami, H. Nakata, Y. Okano, *Langmuir* **2013**, *29*, 2554; b) P. Dhar, T. M. Fischer, Y. Wang, T. E. Mallouk, W. F. Paxton, A. Sen, *Nano Lett.* **2006**, *6*, 66.

[13] C. J. Vessey, J. Wilding, N. Folarin, S. Hirano, M. Takeichi, P. Soutter, G. W. Stamp, M. Pignatelli, *J. Pathol.* **1995**, *176*, 151.

[14] D. J. Wainwright, *Burns* **1995**, *21*, 243.

[15] C. Wang, M. Tammi, R. Tammi, *Histochemistry* **1992**, *98*, 105.

[16] B. A. Dale, K. A. Holbrook, J. R. Kimball, M. Hoff, T. T. Sun, *J. Cell Biol.* **1985**, *101*, 1257.

[17] M. S. Balda, J. A. Whitney, C. Flores, S. Gonzalez, M. Cereijido, K. Matter, *J. Cell Biol.* **1996**, *134*, 1031.

[18] A. Shifren, A. G. Durmowicz, R. H. Knutsen, E. Hirano, R. P. Mecham, *Am. J. Physiol. Lung C* **2007**, *292*, L778.

[19] D. G. Barrett, W. Luo, M. N. Yousaf, *Polym. Chem.* **2010**, *1*, 296.

[20] K. Izumi, J. Song, S. E. Feinberg, *Cells Tissues Organs* **2004**, *176*, 134.

[21] a) D. J. Mooney, H. Vandenburgh, *Cell Stem Cell* **2008**, *2*, 205; b) M. T. Cerqueira, R. P. Pirraco, A. R. Martins, T. C. Santos, R. L. Reis, A. P. Marques, *Acta Biomater.* **2014**, *10*, 3145.

[22] a) J. Yang, M. Yamato, T. Shimizu, H. Sekine, K. Ohashi, M. Kanzaki, T. Ohki, K. Nishida, T. Okano, *Biomaterials* **2007**, *28*, 5033; b) S. Masuda, T. Shimizu, M. Yamato, T. Okano, *Adv. Drug Delivery Rev.* **2008**, *60*, 277.

[23] S. Schacht, Q. Huo, I. G. VoigtMartin, G. D. Stucky, F. Schuth, *Science* **1996**, *273*, 768.

[24] C. L. Marcelo, E. A. Duell, L. M. Rhodes, W. R. Dunham, *J. Invest. Dermatol.* **1992**, *99*, 703.

FULL PAPER